Author Accepted Manuscript version of the paper by Lisa Reis et al.
in 2023 IEEE PES Innovative Smart Grid Technologies Conference Europe - ISGT-Europe (2023),
https://doi.org/10.1109/ISGTEUROPE56780.2023.10407494
Distributed under the terms of the Creative Commons Attribution License (CC BY 4.0)

Applying Vector Fitting for Measurement-based Multiple-Input Multiple-Output Model Identification of a Grid-Forming Converter

[*,#]Lisa Reis
[*]*Dept. of Electrical and Computer Eng.*
RPTU Kaiserslautern-Landau
Kaiserslautern, Germany
reis@eit.uni-kl.de

[§]Andrew Macmillan Smith,
[§]Salvatore D'Arco
[§]*SINTEF Energy Research*
Trondheim, Norway
{andrew.smith, salvatore.darco}@sintef.no

[§,#]Jon Are Suul
[#]*Dept. of Engineering Cybernetics*
NTNU
Trondheim, Norway
jon.are.suul@ntnu.no

***Abstract*—This paper presents an approach for applying Vector Fitting (VF) to identify a small-signal state-space model of a power electronic converter represented as a multiple-input multiple-output (MIMO) system. A workflow for the proposed model identification procedure is presented, with focus on aspects related to the processing of data from measurements and on the configuration of the VF algorithm. An example of how a small-signal state-space model can be identified from laboratory measurements on a $50\,\mathrm{kW}$ grid-forming converter is presented to demonstrate how VF is suitable for identifying black-box MIMO models of power converters. The identification procedure is applied to the full matrix of transfer functions between the input and output combinations obtained from the laboratory measurements. The accuracy of the resulting state-space model is verified in the frequency-domain and by time-domain simulations. Finally, limitations of the presented approach are discussed.**

***Index Terms*—power electronic systems, model identification, state-space models, MIMO systems, laboratory experiments**

I. Introduction

Future power systems will be largely dominated by power electronic converters. To ensure interoperability between the different subsystems, models are needed to assess stability and interaction phenomena. The use of linearized state-space models and eigenvalue methods is common in power system analysis. Moreover, participation factors, mode shapes and eigenvalue sensitivities can provide further insights on the system behaviour [1]. Another advantage is that the state-space model of a large complex system can be assembled from models of the individual components, allowing for a global eigenvalues-based stability assessment [2]. However, detailed information about the structure and parameters of the electrical circuit as well as the control strategy are required for creating analytical state-space models of a power electronic converter.

If only black-boxed models are available, identification methods can be applied to obtain state-space models of power converters [3]. Especially in distribution systems and smart grids, it can be relevant to characterize a converter unit from measurements in a laboratory environment or directly from on-site measurements of a device.

Several previous publications have applied system identification methods to power converters. For instance, the numerical subspace state-space system identification (N4SID) method was utilized to identify a dq-frame model of a VSC with an LCL filter in [4]. In that case, time-domain responses were used to identify the system parameters and eigenvalues, which were further utilized for controller design. A first example of using vector fitting (VF) to find the eigenvalues of a converter unit was presented in [5], for the purpose of apparent impedance analysis of a black-box single-input single-output (SISO) dc system. Furthermore VF has been utilized for sub-system model identification to enable eigenvalue-based stability analysis of converter systems in [6], and [7]. VF is also used in [8] to identify circuit and control parameters in a VSC gray-box model, and this methodology is further extended in [9]. However, all these publications employ simulation models to obtain time or frequency domain data for identification. One example of simulation results supported by experimental data was presented in [10]. This study was based on a cross-correlation identification approach but considered only a SISO system. Thus, model identification of a multiple-input multiple-output (MIMO) system from experimental measurements, or VF-based identification from experimental measurements, have not been previously presented for power electronic systems.

This paper demonstrates the applicability of VF for MIMO model identification of power electronic converters. The presented approach is applied to a converter controlled as a grid-forming unit, by using data from laboratory measurements. The results are obtained from the measurements presented in [11], by improved data processing for generating the input to the VF-based identification. Thus, it is shown how also measurements with low output amplitude at the perturbation frequency, corresponding to low transfer function gain, can be considered in the model identification.

The work was supported by the Ocean Grid Research Project, funded by the Green Platform instrument of the Research Council of Norway under Grant 328750

Author Accepted Manuscript version of the paper by Lisa Reis et al.
in 2023 IEEE PES Innovative Smart Grid Technologies Conference Europe - ISGT-Europe (2023),
https://doi.org/10.1109/ISGTEUROPE56780.2023.10407494
Distributed under the terms of the Creative Commons Attribution License (CC BY 4.0)

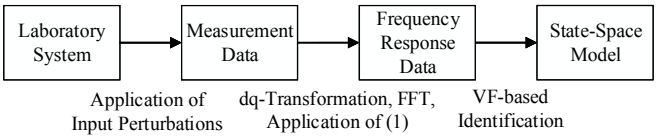

Fig. 1: System identification workflow

Moreover, the paper indicates how to configure the VF algorithm for this specific application.

II. System Identification Workflow

The main steps that have been applied to identify the state-space model of a power electronic converter from measurements are summarized below:

1) Input perturbations are applied to each input and the corresponding response on all outputs is logged.
2) The amplitude and phase of the response for the perturbation frequency in the output is determined by a Fast Fourier Transform (FFT). This is effective to isolate the output response from the noise especially in the case where the amplitude of the response is relatively small.
3) The transfer functions in the frequency domain are extracted for all the combinations of inputs and outputs. The transfer function data $H_{ij}(f_k)$ for the input i and the output j for each frequency f_k is calculated with (1) as the ratio of the Fourier transformation of the output perturbation $Y_{ij}(f_k)$ and the Fourier transformation of the input perturbation $U_i(f_k)$.

$$H_{ij}(f_k) = \frac{Y_{ij}(f_k)}{U_i(f_k)} \tag{1}$$

   The transfer functions are constructed point by point from the collected data.
4) A state-space model is obtained from the experimental data with the VF algorithm. The order of the state-space model is determined by progressively increasing the system order for the VF until the error difference between successive orders is sufficiently low.

The model to be identified is assumed to be operating at an equilibrium in symmetric steady state conditions. For the considered three-phase 2-level (2L) converter, this enables a representation in the synchronously rotating dq-reference frame. This also implies that the input perturbations should be assumed in the rotating reference frame and then transformed to a stationary frame before being applied to the converter. Moreover, stationary frame measurements should be translated into the dq-reference-frame before further processing.

III. Experimental Setup

The laboratory characterization was carried out on a low voltage system configured according to Fig. 2. The setup consists of a $60\,\mathrm{kVA}$ 2L voltage source converter (VSC) with an LCL filter, a star-delta connected transformer with unity voltage ratio and a grid emulator. The grid emulator has 6 output channels with a total power rating of $200\,\mathrm{kVA}$,

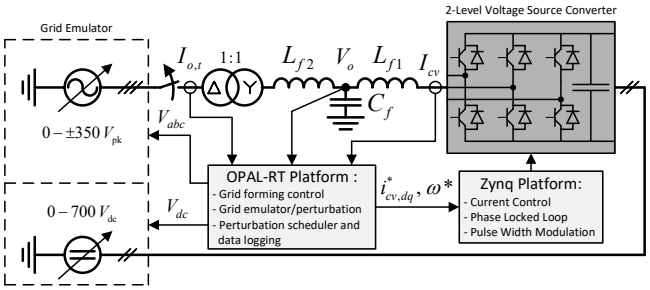

Fig. 2: Schematic view of the experimental setup

wherein 3 channels are utilized to provide the ac-side voltages for the converter under test while 2 channels provide the dc-side voltage. Controlled voltage perturbations can be superimposed to all output channels. The characterization tests were scheduled with an OPAL-RT platform which was also utilized to generate references for the applied perturbations and to log the measurement data [11]. The control and logging was operated at a sampling rate of $100\,\mu\mathrm{s}$.

The studied grid-forming converter is controlled as a virtual synchronous machine (VSM) according to the control scheme documented in [12]. The inner loops (i.e. current control, PLL, Park transformations) are executed on an FPGA-based control board while the the outer-loop controls are implemented on the OPAL-RT platform. The dq-reference frame is aligned with the phase angle of the internal VSM voltage as defined by a virtual swing equation.

The grid-forming converter is assumed as a MIMO dynamic system. The inputs considered for the perturbations are a set of reference signals for the converter (i.e. active and reactive power references, p^*, q^*, voltage and frequency references v^* and ω^*) and the characteristics of the ac voltage applied by the grid emulator (i.e. the grid voltage d- and q-components $v_{\mathrm{g,d}}$ and $v_{\mathrm{g,q}}$ and the grid frequency ω_{g}). The measured outputs are the d- and q-components of the converter current i_{cv}, the output current i_{o} and the the output voltage v_{o}. This leads to seven inputs and six outputs with 42 corresponding input-output transfer functions to be evaluated.

For simplicity, pure sinusoidal perturbations of frequency f_k were applied separately at each individual input i while logging the response on every output j. The tests were performed sequentially for 100 logarithmically spaced frequencies between $0.1\,\mathrm{Hz}$ and $5\,\mathrm{kHz}$. Each disturbance was ramped up from zero to full amplitude within three seconds. The data acquisition was started after another three seconds to ensure the system to be at steady state when data were logged. The logging lasted either one second or at least three periods of the disturbance to provide a sufficiently long logging period. This implies a large collection of measurement data consisting of 4200 data sets with each one corresponding to a point in the transfer functions.

A dq-perturbation at $50\,\mathrm{Hz}$ would cause a dc imbalance in the three-phase system, which could lead to undesired effects due to the delta-winding in the transformer. Therefore,

Author Accepted Manuscript version of the paper by Lisa Reis et al.
in 2023 IEEE PES Innovative Smart Grid Technologies Conference Europe - ISGT-Europe (2023),
https://doi.org/10.1109/ISGTEUROPE56780.2023.10407494
Distributed under the terms of the Creative Commons Attribution License (CC BY 4.0)

TABLE I: Input perturbation amplitudes [11]

Input	**Set-point in p.u.**	$\hat{u}$ **in p.u.**	$k(f)$	**upper limit of** $k(f)$	**frequency range**
p^*	0.2	0.02	1 $0.5 \cdot (f - 5\ \text{Hz})^2 + 1$	- 1000	$\leq$5 Hz >5 Hz
q^*	2	0.1	1	-	all f_k
$v_{\text{g,d}}$	0.95	0.03	1	-	all f_k
$v_{\text{g,q}}$	0	0.03	2 0.5 1	- - -	<0.7 Hz >2 Hz,<50 Hz all other f_k
ω_{g}	1	0.004	1 $0.5 \cdot (f - 5\ \text{Hz})^{0.75} + 1$	- 10	$\leq$7 Hz >7 Hz
ω^*	1	0.04	1 $(f - 5\ \text{Hz})^{1.5} + 1$	- 100	$\leq$5 Hz >5 Hz

measurements between 45 Hz and 55 Hz were omitted. The phase shift of 30° caused by the star-delta connection of the transformer was considered in the calculation of the output quantities by mathematically transforming the voltages to the converter side of the transformer.

IV. Configurations for Applying Vector Fitting

Vector fitting is an open-source algorithm that has been used in many applications for obtaining a state-space model from frequency responses [13]. Vector fitting is known for its ease of use, accuracy in fitting frequency responses, and speed. The frequency response is used to ensure that the system response is captured over a wide range of frequencies. The algorithm has been expanded to handle MIMO systems, called matrix fitting, which is also provided online as open-source code [14].

A main aspect to be considered when identifying models from experimental data is the capability to isolate the output response of the system from the noise. Therefore, the input perturbation amplitude $\hat{u}$ was scaled with a factor $k(f)$, defined as a function of the perturbation frequency according to Table I. Especially for p^*, ω_{g} and ω^* it was necessary to increase the amplitude with increasing frequency, as the integrators in the inertia emulation of the VSM function behave as low pass filters.

The isolation of the output perturbation can be especially challenging when the gain between input and output differs greatly between a subset of outputs combinations. Fig. 3 displays one example measurement for output current and output voltage for a perturbation of the active power reference at 0.1 Hz. In this time domain representation the output perturbation is clearly visible in the d-axis component of the current but difficult to recognize in the d-axis voltage. The effect of the perturbations should therefore be assessed by FFT analysis. However, it should also be considered that logging or measurement errors can cause the predominant input perturbation to slightly deviate from the expected perturbation frequency. Thus, it proved useful to determine which frequency is predominant in the input signal and choose this frequency for the analysis of the output perturbation. As an example, Fig. 4 shows the Fourier spectrum of $v_{\text{o,d}}$ for

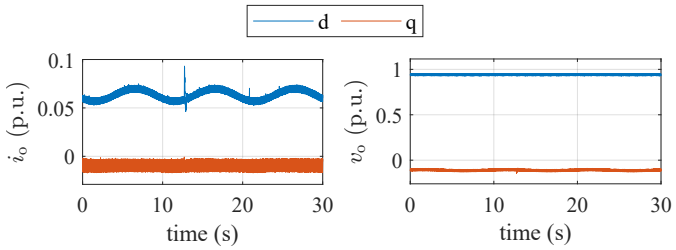

Fig. 3: Measurements for a perturbation of p^* at 0.1 Hz [11]

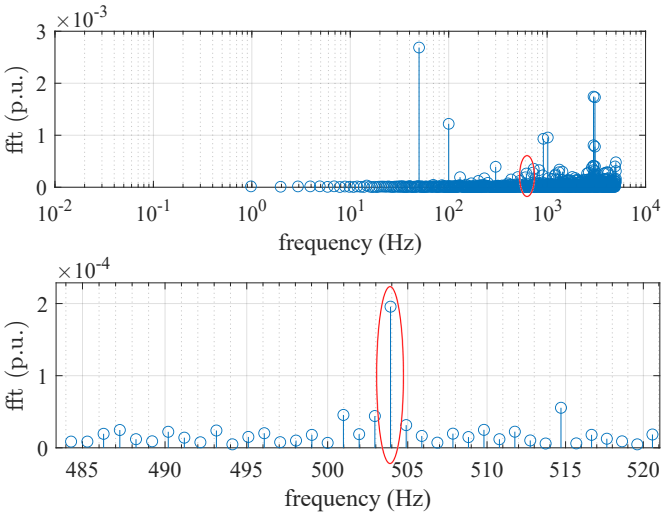

Fig. 4: Fourier spectrum of $v_{\text{o,d}}$ for a perturbation of p^* with 503.7 Hz as a full view (top) and zoomed in on the perturbation frequency (bottom)

a perturbation of p^* with 503.7 Hz. The amplitude of the input perturbation was at 15.7 pu while the output amplitude was $2 \cdot 10^{-4}$ pu resulting in a transfer function magnitude of -100 dB. This confirms how even transfer functions with very low gain can be identified and separated from noise in the measurement data.

As a plausibility check, the calculated transfer function data was compared to the analytical linearized model documented in [12]. The analytical model was parameterized according to the parameters of the test setup. The data for a few selected input-output combinations are displayed in Fig. 5 as an example. Generally, the measurements match well with the overall behaviour of the analytical model. It can be seen that there is a mismatch between the measurements and the analytical model in the upper frequency range. This deviation is assumed to be mainly caused by time delays that are not considered in the the analytical model. Moreover, there are some discrepancies in some of the input-output combinations, especially from $v_{\text{g,d}}$ to the d-components of the current and from $v_{\text{g,q}}$ to the q-components of the current. This is presumably caused by a mismatch between the modelling of the grid impedance in the analytical model and the actual parameters of the laboratory setup.

Based on the measured frequency response curves, VF is used to identify the system model. To move from vector fitting to matrix fitting, which is applicable to MIMO systems,

Author Accepted Manuscript version of the paper by Lisa Reis et al.
in 2023 IEEE PES Innovative Smart Grid Technologies Conference Europe - ISGT-Europe (2023),
https://doi.org/10.1109/ISGTEUROPE56780.2023.10407494
Distributed under the terms of the Creative Commons Attribution License (CC BY 4.0)

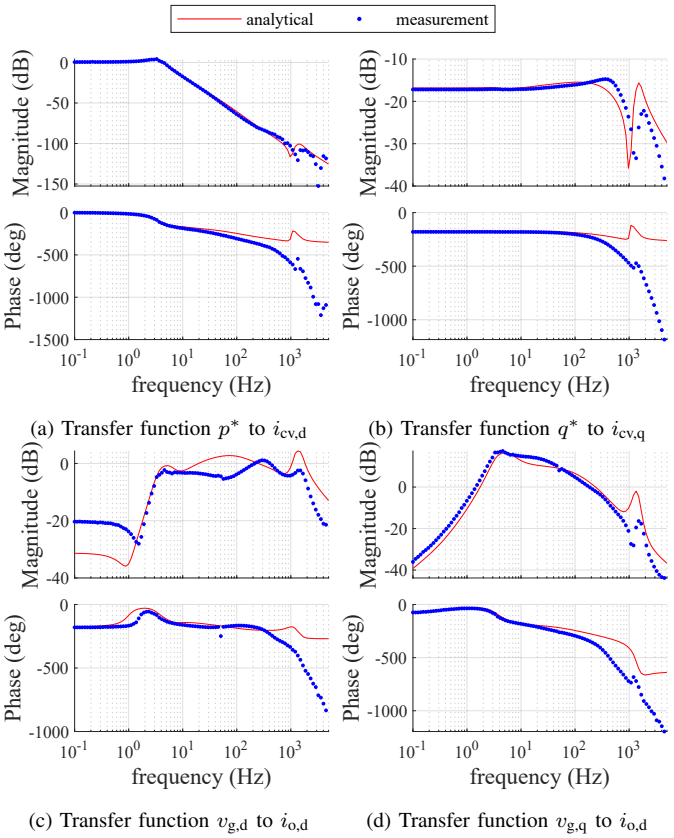

(a) Transfer function p^* to $i_{\mathrm{cv,d}}$ (b) Transfer function q^* to $i_{\mathrm{cv,q}}$

(c) Transfer function $v_{\mathrm{g,d}}$ to $i_{\mathrm{o,d}}$ (d) Transfer function $v_{\mathrm{g,q}}$ to $i_{\mathrm{o,d}}$

Fig. 5: Measurements and analytical results for four examples of input-output combinations

there are some important considerations. Firstly, the original code was developed for square admittance matrices, so some adjustments must be made to the code provided online to allow for systems with unequal numbers of outputs and inputs. Secondly, the weighting applied to the frequency response data plays a critical role in accurately identifying the system. Although any weighting can be defined by the user, there are some suggested weightings accompanying the vector fitting user guide, and the application of the model will determine the best weighting scheme. For example, applying equal or no weighting to all the frequency response data will prioritize larger amplitude responses and therefore fit resonance peaks more accurately. Applying weighting based on the inverse of the amplitude will fit low amplitude phenomena better, which in this case is not advantageous. As the amplitude decreases, the difficulty of extracting data without significant impact from the noise, and the risk of fitting this noise or inaccurate data increases. A weighting with the inverse square-root of the amplitude has been considered as the best compromise in this case, providing a good fit of resonance peaks and high-amplitude phenomena while still capturing low amplitude sections with reasonable accuracy.

V. Identification Results

The identification procedure resulted in the eigenvalues shown in Fig. 6, with an effective order of 12. Note that VF

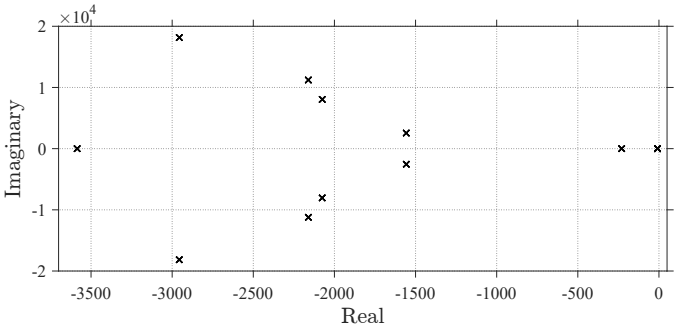

Fig. 6: Eigenvalues of the identified state-space system

repeats the eigenvalues for each input, in this case a total of 7 times.

The frequency responses in the form shown in Fig. 5 were calculated for all 42 input-output combinations and were then utilized for the identification. To examine the accuracy of the identified system model, two approaches are used. The first is visual examination of the accuracy of the frequency responses to the measured values. Additionally, the mean of normalized root mean squared errors (NRMSE) is used to give an overall numerical determination of the goodness of fit. This is a common metric used in MATLAB for comparisons between identification methods, given by the following equation:

$$\mathrm{NRMSE}(\mathbf{H}, \mathbf{H}_0) = \left(1 - \frac{||\mathbf{H}_0 - \mathbf{H}||}{||\mathbf{H}_0 - \mathrm{mean}(\mathbf{H})||}\right) \cdot 100\% \quad (2)$$

where $\mathbf{H}_0$ is the reference data set for the frequency response of one input-output combination and $\mathbf{H}$ the corresponding data set of the fitted system. This definition gives a NRMSE for each input and output combination, which can be examined for each combination individually. However, in this case, the mean of the NRMSEs for all input-output combinations is taken to obtain an overall indication of goodness of fit. The total mean NRMSE for the system is found to be $81.8\,\%$. It should be noted that the NRMSE decreases rapidly as the responses diverge from the measurements, and that $81.8\,\%$ indicates a reasonably good fit.

Fig. 7 shows the bode plot of the measurements and the identified models for four examples of input-output combinations. The errors at the higher frequencies in Fig. 7a appear at very low magnitudes and are therefore assumed to be negligible for the intended use in interoperability analysis.

The second validation approach is conducted in the time domain, by comparison of the step responses. Fig. 8 shows the corresponding step responses for two input-output combinations. The step responses from the identified model matches the measurement well. Indeed, the errors at high frequencies do not have a significant impact on the quality of the step response.

VI. Conclusions

Methods for model identification of power electronic converters are becoming important in the context of assessing potential incompatibilities and interoperability issues without

Author Accepted Manuscript version of the paper by Lisa Reis et al.
in 2023 IEEE PES Innovative Smart Grid Technologies Conference Europe - ISGT-Europe (2023),
https://doi.org/10.1109/ISGTEUROPE56780.2023.10407494
Distributed under the terms of the Creative Commons Attribution License (CC BY 4.0)

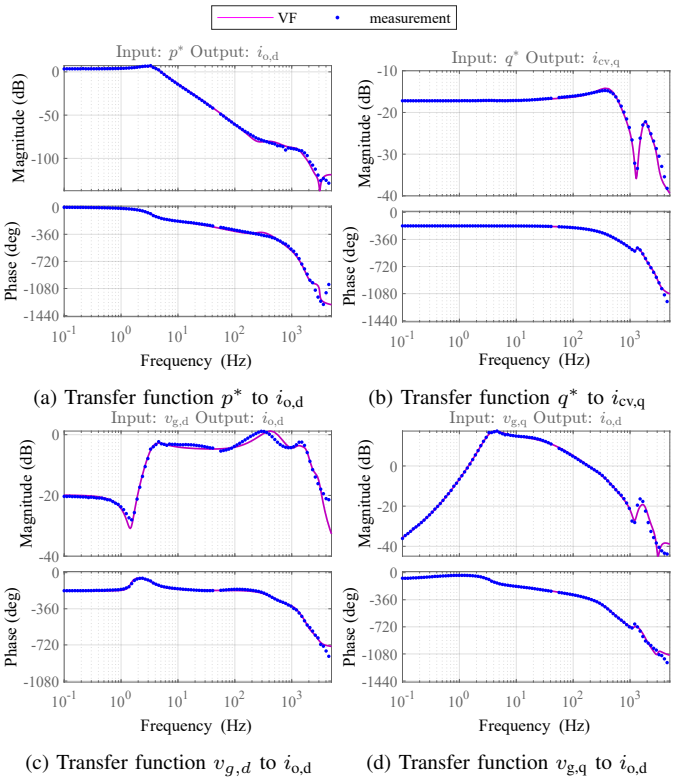

(a) Transfer function p^* to $i_{o,d}$ (b) Transfer function q^* to $i_{cv,q}$

(c) Transfer function $v_{g,d}$ to $i_{o,d}$ (d) Transfer function $v_{g,q}$ to $i_{o,d}$

Fig. 7: Measurements and identification results for four examples of input-output combinations

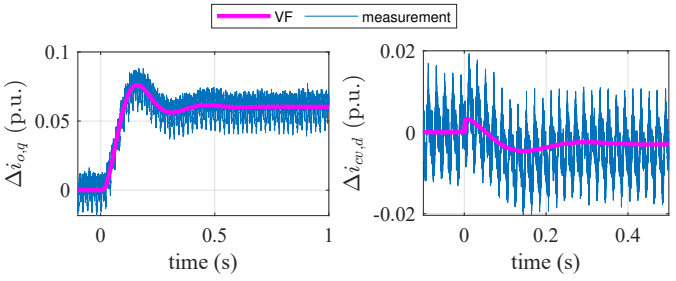

(a) Step in p^* (b) Step in q^*

Fig. 8: Measurement and identification results for two example input-output combinations

access to detailed analytical models. State-space identification methods have been largely developed in the last decades but the application to power electronics is still relatively limited. Moreover, the identification has been normally limited to the output impedance of the converter or equivalently to the input-output transfer function linking the output voltages and currents. In this paper, a complete workflow to identify the state-space model of a power electronic converter as a multiple-input multiple-output (MIMO) system is presented, with focus on the aspects related to processing of data from measurements. By using the example of a grid-forming unit, it is shown that an identification procedure based on vector fitting (VF) is suitable for this application. The resulting state-space model can then be interconnected with state-space models of other parts of a studied power system and utilized for analysis of global small-signal stability. The proposed method does not consider the fact that a perturbation could trigger output perturbations at multiple frequencies (as can be observed for example for a perturbation of $v_{g,q}$ at 0.1 Hz where the dominant frequency in the output $i_{cv,q}$ is double the input perturbation frequency). Thus, further work could include the expansion of the presented method for identifying harmonic state-space models including multiple frequency couplings. This will be necessary for applying the studied identification method to Modular Multilevel Converters (MMCs) and/or power systems operated under unbalanced conditions.

References

[1] P. S. Kundur and O. P. Malik, *Power System Stability and Control*, 2nd ed. McGraw-Hill Education, 2022.

[2] X. Wang and F. Blaabjerg, "Harmonic Stability in Power Electronic-Based Power Systems: Concept, Modeling, and Analysis," *IEEE Transactions on Smart Grid*, vol. 10, no. 3, pp. 2858–2870, May 2019. [Online]. Available: https://ieeexplore.ieee.org/document/8323197/

[3] L. Ljung, *System identification: theory for the user*, 2nd ed., ser. Prentice Hall information and system sciences series. Upper Saddle River, NJ: Prentice Hall PTR, 1999.

[4] F. Huerta, S. Cobreces, F. J. Rodriguez, M. Moranchel, and I. Sanz, "State-space black-box model identification of a voltage-source converter with LCL filter," in *2012 3rd IEEE Int. Symp. on Power Electron. Distr. Gen. Sys. (PEDG)*, Aalborg, Jun. 2012, pp. 550–557.

[5] A. Rygg, M. Amin, M. Molinas, and B. Gustavsen, "Apparent impedance analysis: A new method for power system stability analysis," in *2016 IEEE 17th Workshop on Control and Modeling for Power Electronics (COMPEL)*, Trondheim, Norway, Jun. 2016, pp. 1–7.

[6] M. K. Bakhshizadeh, C. Yoon, J. Hjerrild, C. L. Bak, L. H. Kocewiak, F. Blaabjerg, and B. Hesselbaek, "The Application of Vector Fitting to Eigenvalue-Based Harmonic Stability Analysis," *IEEE Journal of Emerging and Selected Topics in Power Electronics*, vol. 5, no. 4, pp. 1487–1498, Dec. 2017. [Online]. Available: http://ieeexplore.ieee.org/document/7982617/

[7] M. K. Bakhshizadeh, F. Blaabjerg, J. Hjerrild, L. Kocewiak, and C. L. Bak, "Improving the Impedance-Based Stability Criterion by Using the Vector Fitting Method," *IEEE Trans. on Energy Conve.*, vol. 33, no. 4, pp. 1739–1747, Dec. 2018. [Online]. Available: https://ieeexplore.ieee.org/document/8391731/

[8] W. Zhou, Y. Wang, and Z. Chen, "A Gray-Box Parameters Identification Method of Voltage Source Converter Using Vector Fitting Algorithm," in *2019 10th Int. Conf. on Power Electron. and ECCE Asia (ICPE 2019-ECCE Asia)*, Busan, Korea (South), May 2019, pp. 2948–2955.

[9] W. Zhou, R. E. Torres-Olguin, F. Gothner, J. Beerten, M. K. Zadeh, Y. Wang, and Z. Chen, "A Robust Circuit and Controller Parameters' Identification Method of Grid-Connected Voltage-Source Converters Using Vector Fitting Algorithm," *IEEE Journal of Emerging and Selected Topics in Power Electronics*, vol. 10, no. 3, pp. 2748–2763, Jun. 2022. [Online]. Available: https://ieeexplore.ieee.org/document/9354806/

[10] B. Miao, R. Zane, and D. Maksimovic, "System Identification of Power Converters With Digital Control Through Cross-Correlation Methods," *IEEE Trans. on Power Electron.*, vol. 20, no. 5, pp. 1093–1099, Sep. 2005. [Online]. Available: http://ieeexplore.ieee.org/document/1504880/

[11] L. Reis, "Model Identification of Power Electronic Systems for Interaction Studies and Small-Signal Analysis," Master's thesis, University of Kaiserslautern-Landau, Germany, April 2023.

[12] O. Mo, S. D'Arco, and J. A. Suul, "Evaluation of Virtual Synchronous Machines With Dynamic or Quasi-Stationary Machine Models," *IEEE Trans. on Ind. Electron.*, vol. 64, no. 7, pp. 5952–5962, Jul. 2017. [Online]. Available: http://ieeexplore.ieee.org/document/7781612/

[13] B. Gustavsen and A. Semlyen, "Rational approximation of frequency domain responses by vector fitting," *IEEE Transactions on Power Delivery*, vol. 14, no. 3, pp. 1052–1061, Jul. 1999. [Online]. Available: http://ieeexplore.ieee.org/document/772353/

[14] "Matrix Fitting Toolbox." [Online]. Available: https://www.sintef.no/projectweb/vectorfitting/downloads/matrix-fitting-toolbox/